PERFORMANCE ANALYSIS AND DIAGNOSIS OF A PHOTOVOLTAIC MODULE WITH SPONTANEOUS CRACKING

Nicholas Medeiros Lopes[1], Camila Fernanda Cardoso Teixeira[1], Alan Rodrigues de Sousa[1], Dayane Cynthia Pinto Oliveira[1], Amanda Gomes Barboza[1], Samira de Azevedo Santos Emiliavaca[1], João Vitor Fonseca de Mendonça[1], Ana Cleide Bezerra Amorim[1] and João Carlos Lira Neri[1]

[1] SENAI Innovation Institute for Renewable Energy, Natal (Brazil)

Abstract

The reliability of photovoltaic (PV) modules is a key factor in ensuring the long-term efficiency and safety of power plant operations. Spontaneous glass cracks have recently been observed in bifacial silicon modules, though their causes and long-term implications remain unclear. In this study, a cracked monocrystalline silicon bifacial module was analyzed through standard test conditions (STC) performance evaluation, electroluminescence (EL) imaging, and insulation resistance testing, following IEC 61215-2 procedures. Results showed that the module maintained electrical performance consistent with manufacturer specifications, while EL images revealed no evident microcracks or inactive cell regions. Insulation resistance values were within acceptable limits, confirming electrical safety. Although no immediate degradation was detected, the glass cracks may compromise long-term reliability by enabling moisture ingress, promoting hot spot formation, and causing gradual loss of insulation integrity over time.

Keywords: bifacial module, performance STC, eletroluminescence, cracks.

1. Introduction

The reliability of photovoltaic modules is crucial for the sustainable and safe operation of large-scale solar power plants. In such projects, structural or electrical failures in individual modules can result in substantial energy losses, reduce the system's overall efficiency and increase operating costs related to corrective maintenance. In this context, cracks in the glass of modules, particularly bifacial models with glass on both sides, have been identified as a significant issue that directly impacts the durability and return on investment of these installations.

Studies conducted at the Fotovoltaica-UFSC laboratory's experimental plant revealed a high rate of glass breakage in bifacial glass/glass modules, with structural failures occurring after only nine months of operation (Do Nascimento et al., 2024). The analyses identified the reduced thickness of the glass (2 mm), variations outside the manufacturer's specifications, and defects in the interface between the glass and aluminum frame as probable causes. Another case study involving bifacial silicon modules showed that cracks appear spontaneously and continuously with no direct correlation to extreme weather events (De Azevedo et al., 2024).

A review of both studies indicates that the use of materials with lower mechanical resistance, inconsistencies in the manufacturing process, and limitations in the current certification tests can all contribute significantly to cracks forming in photovoltaic modules. In this context, this study aims to assess the impact of these cracks on module performance using analyses based on standardized tests and technical electrical performance criteria.

10.18086/swc.2025.03.49 Available at http://proceedings.ises.org

2. Materials and methodology

2.1 Sample characterization

To estimate the damage caused by the cracks, six commercial photovoltaic module that exhibited spontaneous cracks early in its operation were selected for analysis. One of the modules (Module 1) is based on bifacial monocrystalline silicon technology and has a maximum power output (Pmax) of 540 W under STC, 110 cells (5 x 22), an open-circuit voltage (Voc) of 37.7 V, a short-circuit current (Isc) of 18.3 A, an area of 2.61 m^2 and 2.0 mm back glass thickness, while the other five modules (Modules 2-6) are based on bifacial monocrystalline silicon technology and has a maximum power output (Pmax) of 550 W under STC, 144 cells (6 x 24), an open-circuit voltage (Voc) of 49.6 V, a short-circuit current (Isc) of 14 A, an area of 2.58 m^2 and 2.0 mm back glass thickness. The module was selected due to the presence of visible spontaneous cracks, allowing a real-case scenario investigation into the impact of such defects on energy conversion performance and electrical behavior. Fig 1 illustrates sections of the spontaneous crack observed on the rear glass of the modules, highlighting the extent and pattern of the damage.

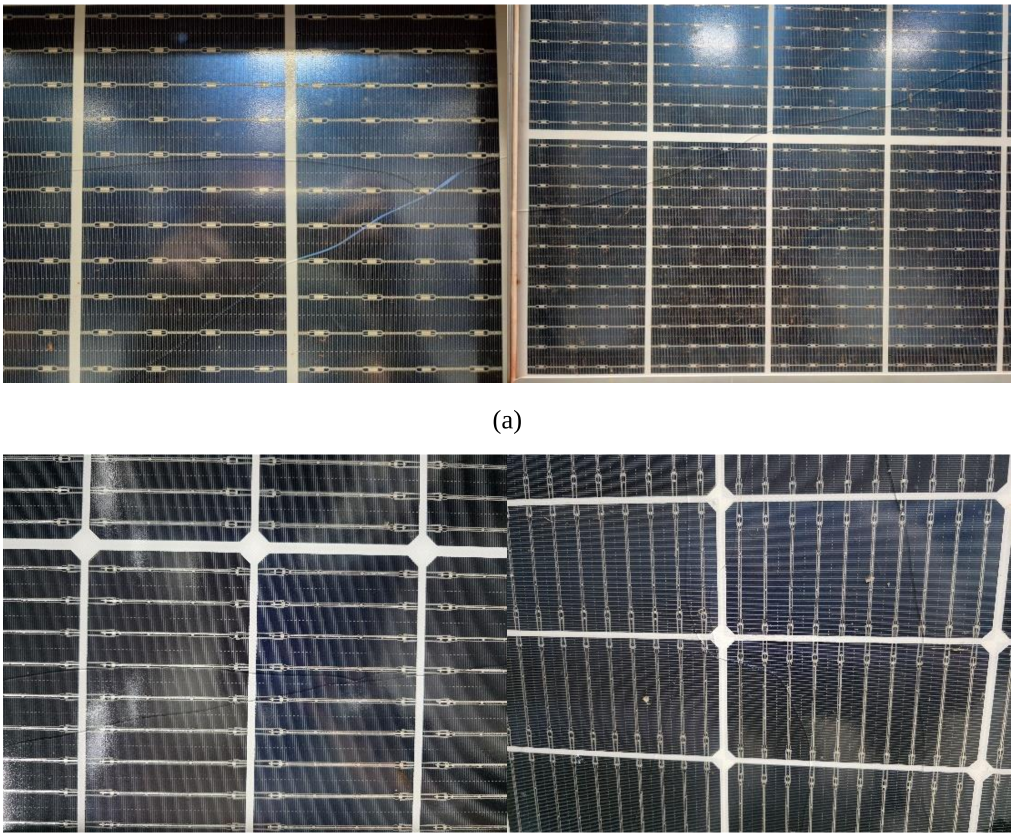

(a)

(b) (c)

Fig. 1: Cracks on the rear of the photovoltaic modules (a) 1, (b) 2 and (c) 3.

2.2 Procedures

The experimental methodology adopted in this study follows the procedures defined by the Brazilian National Institute of Metrology, Quality, and Technology (INMETRO) through Ordinance No. 140/2022, which establishes the Technical Quality Regulation and Conformity Assessment Requirements for photovoltaic (PV) system equipment. This ordinance refers to the international standard IEC 61215-1-2:2021, which specifies the test sequences and methodologies for the design qualification and type approval of crystalline silicon photovoltaic modules.

According to INMETRO Ordinance No. 140/2022 and IEC 61215-1-2:2021, the qualification process involves a series of laboratory tests, including initial stabilization, visual inspection, insulation resistance tests (wet and dry), and maximum power determination. In this work, two of these standardized tests were selected: the maximum power determination and the dry insulation resistance test, as they provide direct indicators of the module's performance and safety following the occurrence of spontaneous cracks.

The maximum power determination test was carried out under Standard Test Conditions (STC) — irradiance of 1000 W/m², spectral distribution AM 1.5G, and cell temperature of 25 °C — using a calibrated solar simulator and an I–V curve tracer. The measured maximum power (Pmax) was compared with the nominal value provided by the manufacturer to quantify the degradation caused by the cracks and to assess the overall efficiency reduction of the module.

The dry insulation resistance test was performed to evaluate the dielectric integrity of the module's insulation system under controlled laboratory conditions. A megohmmeter was used to apply a DC voltage between the module's terminals and its frame, and the resulting resistance was recorded. This procedure allows verification of whether the mechanical damage has compromised the electrical insulation, potentially increasing the risk of leakage currents or electrical hazards.

In addition to these standardized tests, an electroluminescence (EL) imaging analysis was conducted in accordance with IEC 60904-13. The EL technique consists of applying a forward bias current to the module in a dark environment, causing the photovoltaic cells to emit infrared radiation proportional to the local current flow. The emitted radiation was captured by an infrared-sensitive camera, enabling visualization of microstructural defects such as cell cracks, inactive regions, and shunts that may not be observable through visual inspection alone. This diagnostic method provides complementary insight into the physical and electrical integrity of the PV cells, supporting the correlation between visual damage and electrical performance degradation.

The results and analyses obtained from these tests are presented and discussed in Section 3.

3. Results and discussion

3.1 Visual inspection test

The analysis of the results begins with the visual inspection test, during which cracks were identified on the rear surface of the photovoltaic module, as illustrated in Fig. 1. A closer examination revealed that these cracks exhibited continuous propagation across the entire length of the module, extending from one edge to the other. In addition, several secondary branches were observed emerging along the main fracture lines, suggesting a complex pattern of mechanical stress distribution and propagation within the encapsulated structure.

3.2 Insulation test

The insulation resistance test was conducted following the IEC 61215-2 standard, which establishes the procedure for evaluating the electrical insulation of photovoltaic modules. According to this standard, a direct voltage of 1000 V is applied between the active circuit and the grounded frame for a duration of three minutes to assess potential leakage paths and the overall dielectric strength of the module.

As shown in Fig. 2, all tested photovoltaic modules exhibited insulation resistance values well above the minimum requirement of 40 MΩ·m² specified by the standard. These results demonstrate that the presence of spontaneous cracks did not compromise the electrical insulation, indicating that no significant leakage or deterioration occurred during the test.

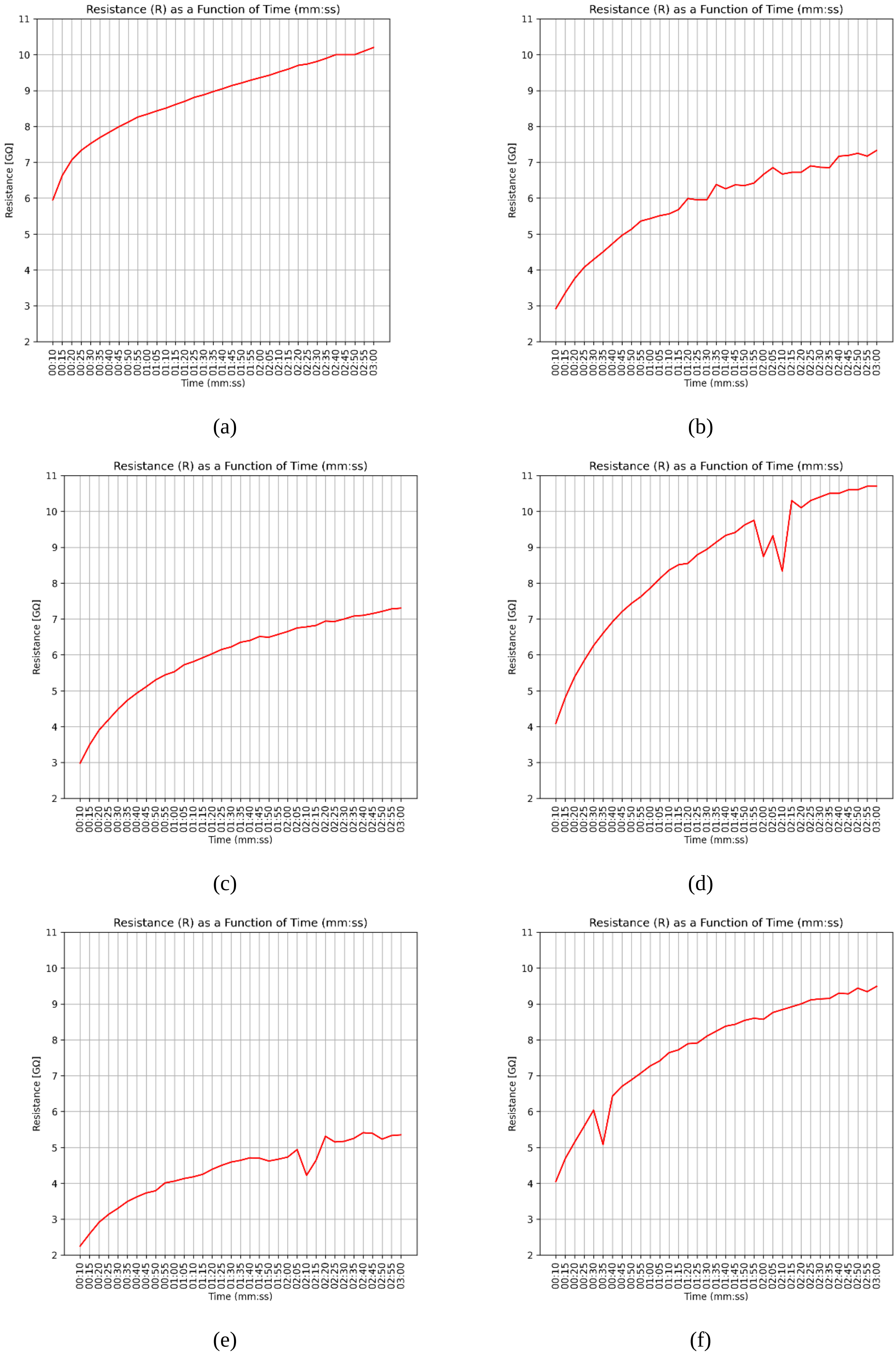

Fig. 2: Insulation tests from the Modules (a) 1, (b) 2, (c) 3, (d) 4, (e) 5 and (f) 6.

3.3 Maximum power determination test

The module performance tests were carried out in accordance with the IEC 61215-2 standard, and the results were compared with the nominal values specified by the manufacturer, as presented in Tables 1 and 2. The tests were performed using a class AAA solar simulator operating under Standard Test Conditions (STC), corresponding to an irradiance of 1000 W/m², a cell temperature of 25 °C, and an air mass (AM) of 1.5 G. During the measurements, the current–voltage (I–V) characteristics were recorded to determine the module's key performance parameters, including maximum power (Pmax), open-circuit voltage (Voc), and short-circuit current (Isc). Despite the presence of visible cracks on the glass surface, the photovoltaic module continued to operate within the expected performance range. The measured values of Pmax, Voc, and Isc showed minimal deviation from the datasheet specifications, demonstrating that the observed mechanical damage did not produce a measurable impact on the module's electrical performance. These findings suggest that the cracks were superficial and did not compromise the integrity or functionality of the solar cells.

Tab. 1: Comparison between manufacture values and those tested in the maximum power test for the 540 W module.

Measurement	Power[W]	Vmpp[V]	Impp[A]	Voc[V]	Isc[A]	Bifaciality[%]
Manufacture	540.00	31.40	17.21	37.70	18.30	70.00
Module 1	542.13	31.17	17.39	37.08	18.40	67.21

Tab. 2: Comparison between manufacture values and those tested in the maximum power test for the 550 W module.

Measurement	Power[W]	Vmpp[V]	Impp[A]	Voc[V]	Isc[A]	Bifaciality[%]
Manufacture	550.00	41.70	13.20	49.60	14.00	70.00
Module 2	531.67	41.75	12.74	49.88	13.45	71.13
Module 3	537.49	41.65	12.90	49.98	13.54	71.70
Module 4	536.12	41.76	12.84	49.97	13.56	71.50
Module 5	534.51	41.70	12.82	49.96	13.42	71.71
Module 6	536.16	41.57	12.90	49.80	13.51	69.31

Fig. 3 presents the individual current–voltage (I–V, in black) and power–voltage (P–V, in red) characteristics measured for both the front and rear sides of the photovoltaic module. The results demonstrate a strong agreement with the nominal data, indicating consistent electrical behavior under standard test conditions. As expected, the rear-side measurements exhibit slightly lower values due to partial shading caused by the metallic frame and the junction box, which limit the effective irradiance on the rear surface. Similar to the findings of the insulation resistance test, the module remains fully operational and maintains its expected efficiency, confirming that the presence of surface cracks did not lead to any measurable degradation in its performance.

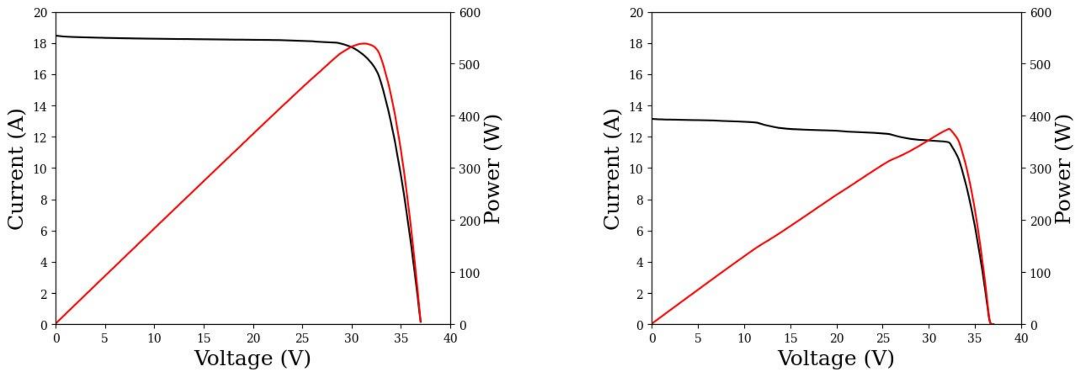

(a) (b)

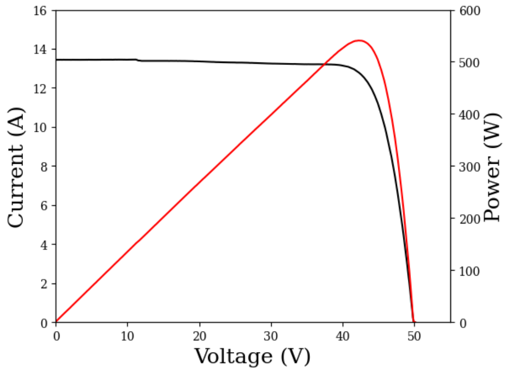
Current (A)
Power (W)
Voltage (V)

(c)

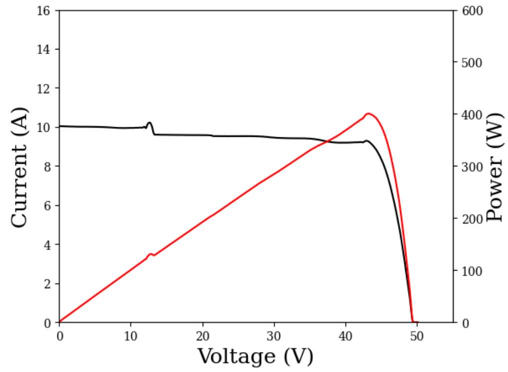
Current (A)
Power (W)
Voltage (V)

(d)

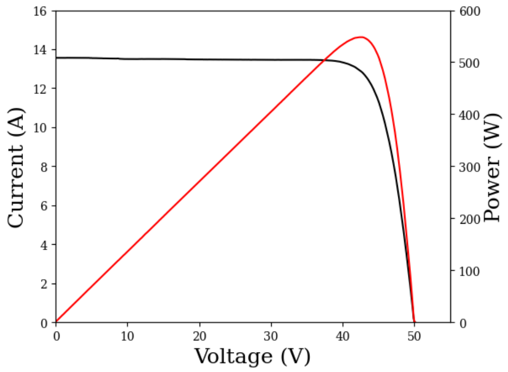
Current (A)
Power (W)
Voltage (V)

(e)

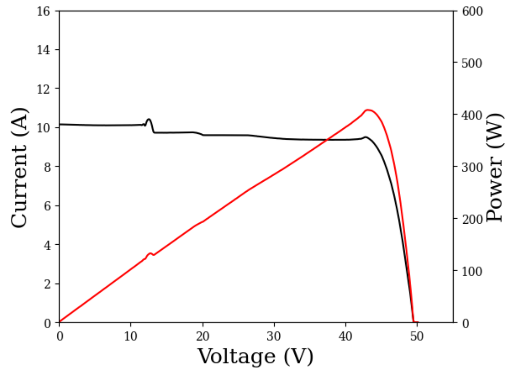
Current (A)
Power (W)
Voltage (V)

(f)

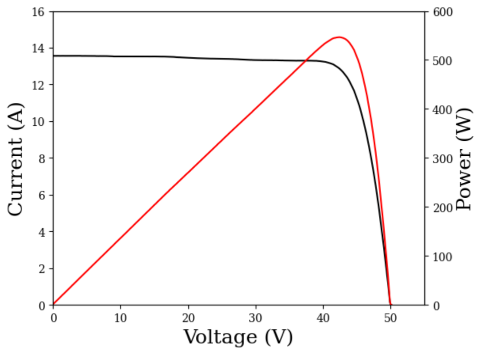
Current (A)
Power (W)
Voltage (V)

(g)

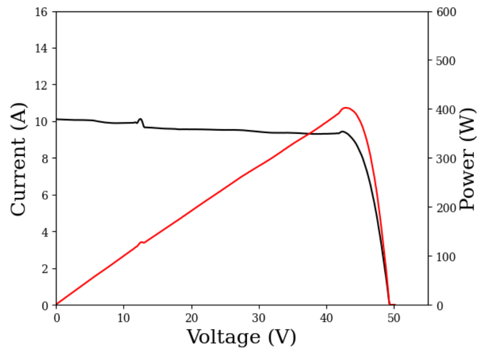
Current (A)
Power (W)
Voltage (V)

(h)

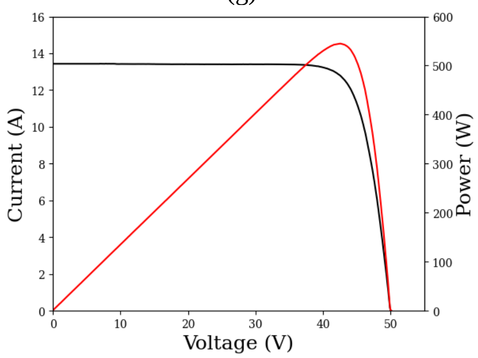
Current (A)
Power (W)
Voltage (V)

(i)

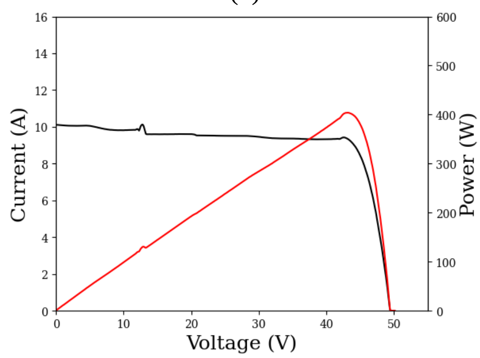
Current (A)
Power (W)
Voltage (V)

(j)

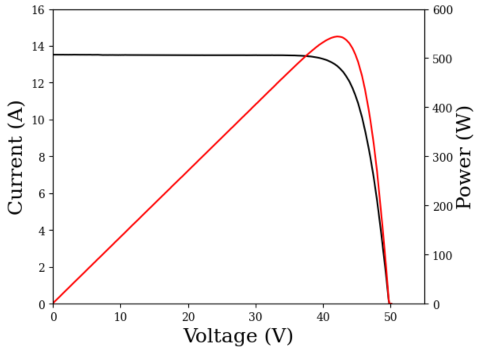

(k)

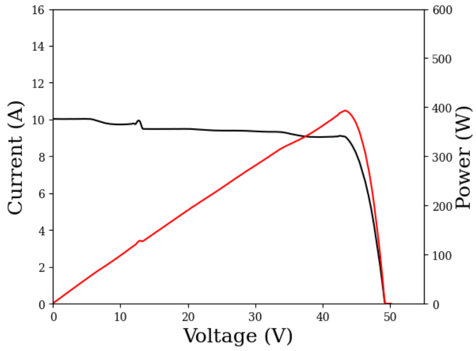

(l)

Fig. 3: I-V and P-V curve measurements performed on module 1 (a) front and (b) rear surfaces, module 2 (c) front and (d) rear surfaces, module 3 (e) front and (f) rear surfaces, module 4 (g) front and (h) rear surfaces, module 5 (i) front and (j) rear surfaces and module 6 (k) front and (l) rear surfaces.

3.4 Electroluminescence test

The electroluminescence (EL) imaging test was conducted to evaluate the internal condition of the photovoltaic module and identify possible microcracks or inactive regions within the solar cells. As presented in Fig. 4, no signs of electrical damage were detected in the areas corresponding to the visible cracks on the glass surface. The EL image revealed uniform luminescence without dark regions or disruptions in the emission pattern, indicating that the mechanical cracks were confined to the glass layer and did not propagate into the silicon cells. Consequently, the structural integrity and electrical continuity of the cells remained unaffected by the observed surface defects.

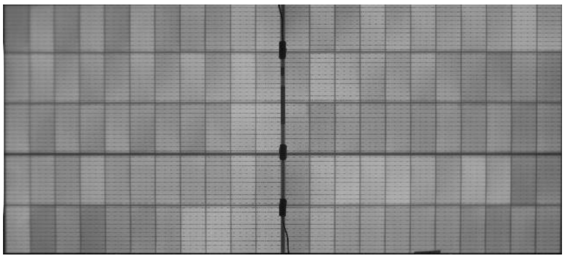

(a)

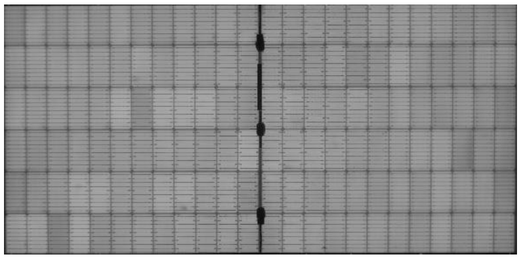

(b)

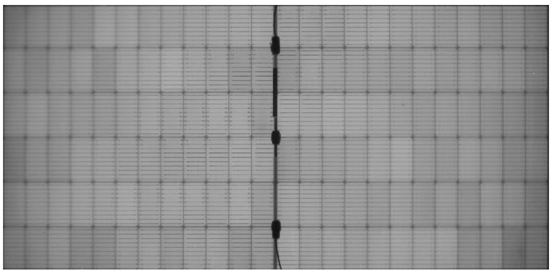

(c)

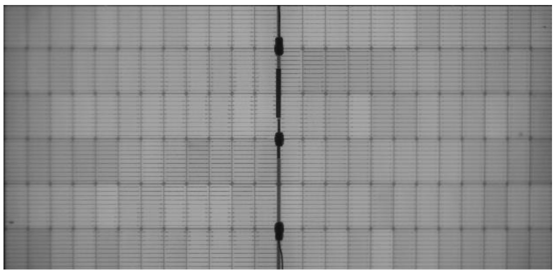

(d)

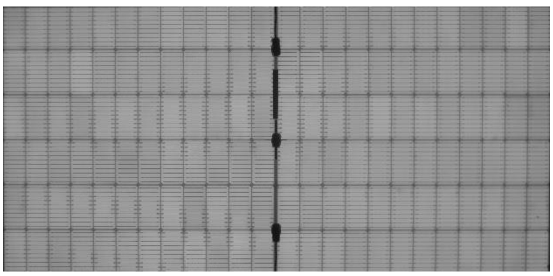

(e)

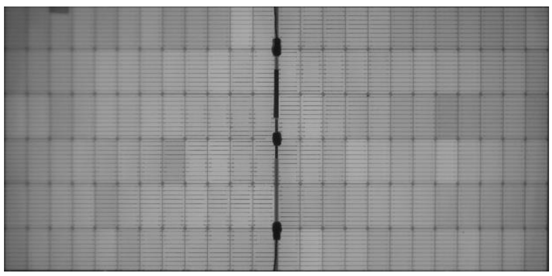

(f)

Fig. 4: EL of the rear side of the PV modules(a) 1, (b) 2, (c) 3, (d) 4, (e) 5 and (f) 6.

3.5 Before spontaneous cracks comparison

Prior to the occurrence of spontaneous cracks in the photovoltaic module 3 presented on this article, the same testing methodology applied to the damaged modules was also conducted on this unit in its intact condition. This procedure allows for a direct and reliable comparison between the electrical and physical characteristics of the module before and after the cracking event. By maintaining identical test conditions and measurement parameters, the influence of the spontaneous cracks on the module's performance can be accurately assessed and isolated from other external variables.

Fig. 5 shows the comparison between the insulation resistance test performed before and after the appearance of cracks. The results demonstrate that, even after the occurrence of the cracks, the insulation resistance remains above the acceptable threshold defined for the module. This indicates that the mechanical damage did not immediately compromise the module's electrical insulation integrity.

(a) (b)

Fig. 5: Insulation test of the Module 3 (a) beore and (b) after the cracks.

Fig. 6 presents the comparison of the maximum power determination test conducted on the front and rear sides of the modules before and after the appearance of cracks. The results show that the presence of cracks did not cause a significant reduction in power output on either side of the module. This indicates that, at this stage, the cracks in the glass do not immediately affect the electrical performance of the cells.

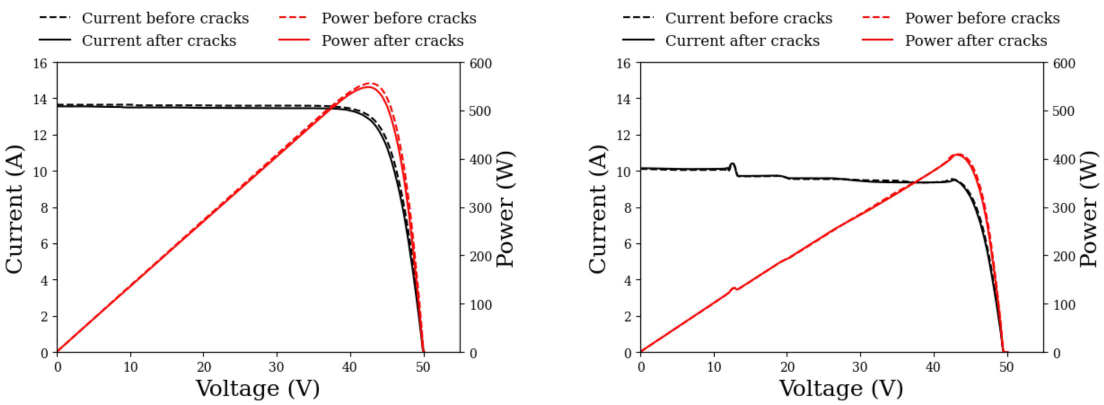

(a) (b)

Fig. 6: Maximum power determination test from Module 3 (a) front and (b) rear sides.

Fig. 7 presents the results of the electroluminescence (EL) tests conducted before and after the appearance of cracks. The images show that, despite the visible cracks in the glass, no damage or microcracks were detected in the solar cells, indicating that the electrical integrity of the module remained intact. These findings are consistent with the maximum power test results, which showed no performance degradation at this initial stage. This suggests that the degradation process occurs gradually, with potential impacts on power output and efficiency becoming evident only over time. Moreover, this phenomenon has been increasingly reported in large-scale photovoltaic power plants, where spontaneous glass cracks do not immediately affect electrical performance and are therefore undetectable through remote monitoring systems, requiring detailed on-site visual inspections for identification.

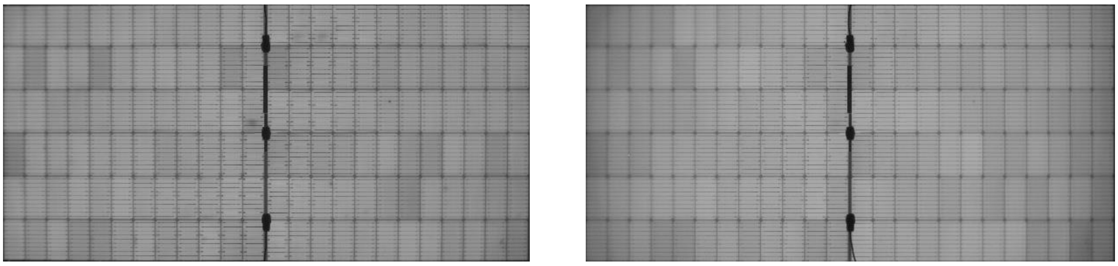

(a) (b)

Fig. 7: EL picture of the Module 3 (a) before and (b) after the cracks.

4. Conclusion

The results indicated that, despite the rear glass crack, the module's electrical behavior remained within the manufacturer's specified parameters. The I-V curve showed no anomalies, and maximum power output was within the expected tolerance. Insulation tests also confirmed compliance with safety standards, with no faults between active circuits and the metal frame.

Electroluminescence imaging revealed no cell cracks, suggesting the damage was limited to the surface encapsulation. However, such cracks still pose long-term risks. Over time, exposure to humidity, thermal cycles, and contaminants can accelerate degradation, potentially leading to hot spots, insulation failures, and inverter shutdowns. These issues often go undetected in routine inspections and require detailed diagnostics like EL imaging. Therefore, the study emphasizes the need for regular monitoring to detect early-stage defects that may later affect system performance and reliability.

5. Acknowledgements

This research was carried out as part of the activities of the National Institute for Technological Development of Photovoltaic Solar Energy Applications (INCT-DAESF), funded by the Brazilian agencies CNPq and MCTI under process number 408486/2024-4. The authors would like to thank the SENAI Institute for Innovation in Renewable Energy for its support and infrastructure; CTG Brazil, for its financial contribution to the ANEEL PD-10381-0620/2020 project; and TotalEnergies, for its current financial contributions to the ANP 23980-6 and ANP 24118-2 projects. The authors would like to thank ISI-ER for their support in the development of this work and TotalEnergies for the current financial support under the ANP PD-24118-2 project.

6. References

BRASIL. Instituto Nacional de Metrologia, Qualidade e Tecnologia (Inmetro). Portaria nº 140, de 25 de março de 2022. Regulamento Técnico da Qualidade e Requisitos de Avaliação da Conformidade para Equipamentos de Sistemas Fotovoltaicos. Brasília, 2022.

De Azevedo, K.L.R., Braga, M., Rüther, R., 2024. Estudo de caso sobre incidência e padrões de trincas em módulos fotovoltaicos de silício bifaciais vidro-vidro de grande área, in: Anais Congresso Brasileiro de Energia Solar – CBENS 2024.

Do Nascimento, B., et al., 2024. Análise da espessura dos vidros e da interface moldura-vidro em módulos fotovoltaicos bifaciais com uso de microscopia eletrônica de varredura, in: Anais Congresso Brasileiro de Energia Solar – CBENS 2024.

IEC – International Electrotechnical Commission. IEC 61215-1-1:2021 – Terrestrial photovoltaic (PV) modules – Design qualification and type approval – Part 1-1: Special requirements for testing of crystalline silicon photovoltaic (PV) modules. Geneva: IEC, 2021.

IEC – International Electrotechnical Commission. IEC 61215-2:2021 – Terrestrial photovoltaic (PV) modules – Design qualification and type approval – Part 2: Test procedures. Geneva: IEC, 2021.

IEC - International Electrotechnical Commission, 2018. IEC TS 60904-13: Photovoltaic devices – Part 13: Electroluminescence of photovoltaic modules.